

---

# Mouse Barrel Cortex Functionally Compensates for Deprivation Produced by Neonatal Lesion of Whisker Follicles

---

Peter Melzer, Alison M. Crane and Carolyn B. Smith

Laboratory of Cerebral Metabolism, National Institute of Mental Health, Bldg 36, Room 1A05, 9000 Rockville Pike, Bethesda, MD 20892, USA

*Key words:* neonatal plasticity, mouse, barrel cortex, quantitative autoradiographic deoxyglucose method

## Abstract

In the murine somatosensory pathway, the metabolic whisker map in barrel cortex derived with the autoradiographic deoxyglucose method is spatially in register with the morphological whisker map represented by the barrels. The barrel cortex of adult mice, in which we had removed three whisker follicles from the middle row of whiskers shortly after birth, contained a disorganized zone surrounded by enlarged barrels with partially disrupted borders. With the fully quantitative autoradiographic deoxyglucose method, we investigated in barrel cortex of such mice the magnitude and the pattern of metabolic responses evoked by the deflection of whiskers. Most remarkably, the simultaneous deflection of six whiskers neighbouring the lesion activated not only the territory of the corresponding barrels, but also the unspecifiable area intercalated between the clearly identified barrels. This metabolic whisker map, unpredictable from the morphological 'barrel' map, may reflect a functional compensation for the deficit in input.

## Introduction

The rodent whisker-to-barrel pathway is the part of the somatosensory system that connects whisker follicles on the snout via synaptic relays in the brainstem and, across the midline, in the thalamus with that area of neocortex known as 'barrel cortex'. Barrels appear in layer IV as rings of cell bodies, 'sides', surrounding neuropil-rich centres, the 'hollows' and separated by cell body-sparse 'septa' (Woolsey and Van der Loos, 1970). Barrels represent the whiskers on the snout topologically, the whisker map being inverted about the longitudinal axis. Barrels develop in the first postnatal week, and their morphology can be manipulated by the selective lesion of whisker follicles until they are formed (Van der Loos and Woolsey, 1973; Killackey and Belford, 1979; Jeanmonod *et al.*, 1981; Durham and Woolsey, 1984). The earlier the follicles are removed, the more extensive is the resulting morphological aberration (Jeanmonod *et al.*, 1981). Lesions within the first 2 days after birth lead to the development of enlarged barrels surrounding a disorganized zone in place of the barrels that would have represented the removed follicles. Thus it appears that the rodent whisker-to-barrel pathway exhibits plasticity during a critical period in development exemplified by abnormal cortical morphology resulting from a peripheral insult. Electrophysiological recordings from anaesthetized rats and mice indicate that cortical neurons in the disorganized zone are unresponsive to stimulation of remaining whiskers (Simons *et al.*, 1984). In contrast, in primates monocular

deprivation during a critical period leads to the *complete* invasion of the deprived territory in primary visual cortex by input from the intact eye (Hubel *et al.*, 1977; Des Rosiers *et al.*, 1978).

To resolve this discrepancy in findings, we examined in the present study the functional ramifications of the morphological changes in barrel cortex induced by neonatal follicle lesions. The autoradiographic [<sup>14</sup>C]deoxyglucose method (Sokoloff *et al.*, 1977), which determines simultaneously rates of glucose utilization in all regions of the brain, was used for this purpose. Because regional neural spiking activity and energy metabolism are closely linked (Sokoloff, 1985), the deoxyglucose method permits the qualitative and quantitative assessment of stimulus-related metabolic responses in a sensory pathway. We have applied this technique to investigate in adult mice whether the territory in barrel cortex which had been deprived of its sensory input by the removal of whisker follicles shortly after birth could be metabolically activated by the deflection of whiskers adjacent to the lesion. If so, how would the pattern of activation compare with the morphological adaptations to the lesion? Our results provide evidence for a functional reorganization of the mouse barrel cortex following the neonatal lesion of whisker follicles by demonstrating that the territory which would have represented the removed whisker follicles does respond to the simultaneous deflection of six whiskers adjacent to the lesion with an increase in energy metabolism.

## Materials and methods

### Animals

All procedures were in strict accordance with the National Institutes of Health Guide for the Care and Use of Laboratory Animals and were approved by the NIMH Animal Care and Use Committee. Female and male Swiss albino mice of ICR origin were purchased from Harlan Sprague–Dawley, Indianapolis, IN, USA. Pregnant females were checked for offspring at noon daily. Both male and female pups were included in the study. The experiments are listed in Table 1. Whisker follicles were removed from seven pups within 8 h of noting their birth, i.e. on postnatal day 0, and four pups within 30–31 h of noting their birth, i.e. on postnatal day 1. The time of lesion in each experiment is given in Table 2. Pups were cooled on ice, and an incision was made ventral and posterior to the middle row of whiskers on the left side of the snout. The large whiskers are arrayed in five rows, named A (dorsal) to E (ventral). In each row, the whiskers are numbered in rising sequence beginning posteriorly. Four single whiskers,  $\alpha$  (dorsal) to  $\gamma$  (ventral), straddle the rows' caudal ends (Woolsey and Van der Loos, 1970). The follicles of whiskers C1, C2 and C3 were excised. Pups were allowed to recover from the surgery under a heat lamp, after which they were returned to their mothers. Pups with lesions were reared with unoperated littermates under standard laboratory conditions of a 12/12 h light/dark cycle. The litters were weaned 4 weeks after birth. The mothers as well as the weaned mice had access to food and water *ad libitum*. The mice were 14 weeks and older when they were subjected to the whisker-stimulation experiment. Unoperated littermates and normal mice older than 6 weeks served as controls. Left whiskers B1–3 and D1–3 were stimulated in nine animals with the lesion and in 14 controls (Table 1). In two experiments whisker D3 detached shortly after stimulation had begun (LES.05 and NOR.14). In three mice with the lesion the following whiskers were stimulated: whisker  $\gamma$  (LES.12), whiskers D2 and D3 (LES.08) and whiskers  $\gamma$  and D3 (LES.11).

### Preparation of animals

Polyethylene catheters were inserted into a femoral vein and artery under light halothane anaesthesia (~1.5% in 70% N<sub>2</sub>O/30% O<sub>2</sub>). Catheters were threaded under the skin to exit at the nape of the neck, and the wound was sutured. Pieces of Ni/Fe wire (0.2 mm in diameter and 2.5 mm long) were glued on the selected whiskers on the left side of the snout ~5 mm above the surface of the skin, and the whiskers were clipped distal to the ends of the wires. All other whiskers, left and right, were clipped close to the skin surface. Paper collars were fitted around the animals' necks to prevent the mice from removing the wires. They were allowed to recover from anaesthesia for 16–24 h and provided with food and water *ad libitum*. On the day of the experiment, the mice were momentarily immobilized with 2% halothane, a small incision was made at the nape of the neck, and the catheters were exposed. This procedure took <5 min. Mice were placed in a small glass box inside the stimulator and allowed to rest for 45 min, a time span long enough for them to recover completely from any effects of the whiff of halothane.

### Physiological variables

Arterial blood pressure and haematocrit were determined just prior to and again 40 min after the deoxyglucose injection. Arterial blood pH and blood gas tensions were determined at 45 min. Arterial plasma glucose concentration was measured at various times throughout the experiment.

Mean arterial blood pressure was measured by means of an

TABLE 1. Summary of experimental details

Code <sup>a</sup>	Sex <sup>b</sup>	Age <sup>c</sup> (months)	Stimulated whiskers <sup>d</sup> (left side)	Histology <sup>e</sup>		
				cortex	Whiskerpads	
					left	right
LES.01	M	3.5	B1–3 and D1–3	CO/N <sup>3-D</sup>	W/L	W/L
LES.02	F	4.5	B1–3 and D1–3	CO/N <sup>3-D</sup>	W/L	W/L
LES.03	F	4.0	B1–3 and D1–3	CO/N	W/L	W/L
LES.04	F	5.5	B1–3 and D1–3	CO/N <sup>3-D</sup>	W/L	W/L
LES.05	F	5.5	B1–3 and D1–2*	CO/N <sup>3-D</sup>	W/L	W/L
LES.06	M	3.5	B1–3 and D1–3	CO/N <sup>3-D</sup>	W/L	W/L
LES.07	F	4.5	B1–3 and D1–3	CO/N <sup>3-D</sup>	W/L	W/L
LES.08	F	12.0	D2 and D3	CO/N <sup>3-D</sup>	W/–	W/–
LES.09	F	13.0	B1–3 and D1–3	CO/N <sup>3-D</sup>	L/L	L/L
LES.10	M	6.0	B1–3 and D1–3	CO/N <sup>3-D</sup>	W/L	W/L
LES.11	F	13.0	$\gamma$ and D3	CO/N <sup>3-D</sup>	L/L	L/L
LES.12	M	13.5	$\gamma$	CO/N <sup>3-D</sup>	L/L	L/L
NOR.01	M	1.5	B1–3 and D1–3	N	W/–	W/–
NOR.02	M	1.5	B1–3 and D1–3	N	W/–	W/–
NOR.03	M	2.0	B1–3 and D1–3	N	W/–	W/–
NOR.04	M	2.5	B1–3 and D1–3	N	W/–	W/–
NOR.05	M	2.5	B1–3 and D1–3	N		
NOR.06	M	2.5	B1–3 and D1–3	N		
NOR.07	M	2.5	B1–3 and D1–3	N		
NOR.08	F	10.0	B1–3 and D1–3	CO	W/–	W/–
NOR.09	F	11.5	B1–3 and D1–3	CO <sup>3-D</sup>	W/L	W/L
NOR.10	F	12.0	B1–3 and D1–3	CO	–/L	W/–
NOR.11	F	13.5	B1–3 and D1–3	CO/N <sup>3-D</sup>	L/L	L/L
NOR.12	F	14.0	B1–3 and D1–3	CO/N <sup>3-D</sup>	L/L	L/L
NOR.13	F	14.0	B1–3 and D1–3	CO/N <sup>3-D</sup>	L/L	L/L
NOR.14	M	12.0	B1–3 and D1–2*	CO/N <sup>3-D</sup>	–/L	–/L

<sup>a</sup>Operated mice and unoperated controls are coded with the prefixes LES and NOR respectively. The number following the prefix identifies the particular experiment. <sup>b</sup>M, male; F, female. <sup>c</sup>Age of animal at which deoxyglucose experiment was carried out. <sup>d</sup>Apart from LES.12 (one whisker), LES.11 and LES.08 (two whiskers), the mice had six whiskers stimulated in the deoxyglucose study. In the experiments labelled with asterisks whisker D3 detached shortly after stimulation had begun. <sup>e</sup>Sections through cortex were stained for cytochrome oxidase (CO) activity or for Nissl (N). 3-D labels material used for three-dimensional reconstructions. Sections through whiskerpads were stained with Liesegang's (L) or with Weil's (W) method; blank indicates that whiskerpads were not kept; – indicates that second section series were not available.

air-damped mercury manometer. Arterial blood pH, pO<sub>2</sub> and pCO<sub>2</sub> were measured with a Corning 158 pH/Blood Gas Analyser (Corning Ltd, Halstead, Essex, UK). Arterial blood haematocrit was determined in blood samples collected in capillary tubes which were subsequently sealed and centrifuged. Arterial plasma glucose concentrations were measured with a Beckman Glucose Analyzer 2 (Beckman Instruments, Fullerton, CA, USA). The means and standard deviations for these variables were as follows: haematocrit 41 ± 3%, blood pressure 86 ± 11 mm Hg, pH 7.24 ± 0.08, pO<sub>2</sub> 85.1 ± 8.0 torr, pCO<sub>2</sub> 39.8 ± 5.5 torr, and glucose concentration 6.5 ± 2.2 mM.

### Measurement of local cerebral glucose utilization

The whiskers with metal pieces were stimulated by exposing the mice to a pulsating magnetic field (Melzer *et al.*, 1985). The experimental procedure was initiated by the simultaneous onset of the magnetic field and the intravenous pulse of 2-deoxy-D-[1-<sup>14</sup>C]glucose (specific activity, 50–55 mCi/mmol, DuPont–NEN, Wilmington, DE, USA; dose 120–150  $\mu$ Ci/kg) in ~40  $\mu$ l heparinized saline (Sokoloff *et al.*, 1977). Whisker stimulation was maintained for the entire duration of the experiment. Timed arterial 20  $\mu$ l blood samples were drawn throughout the entire experiment interval. The samples were immediately centrifuged to separate the plasma, and plasma concentrations of [<sup>14</sup>C]deoxyglucose and glucose were measured. Concentrations of <sup>14</sup>C were assayed by means of a TRI-CARB Liquid Scintillation Analyzer,

Model 2000CA (Packard Instrument Co., Downers Grove, IL, USA) with external standardization. The mice were killed at precisely recorded times between 46 and 55 min after the pulse of [ $^{14}\text{C}$ ]deoxyglucose. The brains were rapidly removed, and the forebrain was separated from the brainstem and divided into the hemispheres. The tissues were then frozen in isopentane chilled to  $-55^\circ\text{C}$  with dry ice and stored at  $-70^\circ\text{C}$  until processed for autoradiography. Serial sections of neocortex ( $20\ \mu\text{m}$  in thickness) were cut tangentially to the pial surface in a cryostat maintained at  $-22^\circ\text{C}$ . The sections were collected on chilled ( $-22^\circ\text{C}$ ) gelatin-coated slides and dried on a hotplate at  $60^\circ\text{C}$ . When an alternate section series was collected, the additional series was dried at room temperature. The hotplate-dried sections were autoradiographed along with calibrated [ $^{14}\text{C}$ ]methylmethacrylate standards on Kodak OMC1 X-ray film at  $4^\circ\text{C}$  for 1–12 weeks. In some unoperated controls only hotplate-dried section series were prepared. After autoradiography, these series were stained for either cytochrome oxidase activity (Wong-Riley, 1979) or Nissl substance with thionin. In mice in which two section series were obtained, one series was stained for Nissl substance and the other was stained for cytochrome oxidase activity. The histological methods employed in each experiment are listed in Table 1.

Optical densities in autoradiograms were measured by means of a CCD camera-based computerized image-processing system (Imaging Research, St Catharines, Ontario, Canada). In order to select regions of interest, outlines of the barrels were drawn on digitized images of the cytochrome oxidase-stained sections of cortex and stored as bitmaps by means of the image-processing system. In those cases in which only Nissl-stained preparations were available, outlines of the barrels were drawn with a computer-assisted microscope (MicroBrightField, Baltimore, MD, USA, and Wild & Leitz, Wetzlar, FRG) and stored as bitmaps. The digitized drawings were superimposed on the images of the autoradiograms, which had also been digitized with the camera-based image-processing system, and used to outline the regions of interest on the autoradiograms. The  $^{14}\text{C}$  concentration in each region was determined by comparing the optical densities measured in the autoradiograms with optical densities derived from a set of calibrated standards autoradiographed on the same X-ray film. The pixel-weighted averages of the local tissue  $^{14}\text{C}$  concentrations were used to calculate rates of glucose utilization with the operational equation of the method of Sokoloff *et al.* (1977). In this calculation we employed the rate constants ( $k_1^* 0.189$ ,  $k_2^* 0.245$  and  $k_3^* 0.052$ ) and the lumped constant (0.483) determined for the normoglycaemic, conscious rodent (Sokoloff *et al.*, 1977). For hypoglycaemic animals, i.e. mice with plasma glucose concentrations  $<4.4\ \text{mM}$  (LES.09, LES.11, NOR.08, NOR.10 and NOR.12), the lumped constant was adjusted as described by Suda *et al.* (1990).

Rates of glucose utilization were determined in five areas of barrel cortex in both hemispheres: the barrels representing whiskers A1–3, B1–3, C1–3, D1–3 and E1–3. In the mice in which the follicles of whiskers C1–3 had been removed, the area between the enlarged barrels of rows B and D, henceforth named 'disorganized zone', was taken as homeotopic to barrels C1–3. In some mice that territory contained poorly defined barrels (see below). In such cases, including the mice with one or two stimulated whiskers, the anterior compartment did not show increased rates of glucose utilization and was measured separately from the posterior compartment(s). Mice LES.05 and NOR.14, which had lost a whisker during stimulation, were excluded from quantification. Three-dimensional reconstructions of metabolic activity in the right hemisphere were generated for unoperated as well as for operated mice (Table 1) with the image-processing software package IMAGE (provided by W. Rasband, NIMH, USPHS, Bethesda, MD, USA). The autoradiogram of every second section through the

cortical hemisphere was used for this purpose. The images were brought in register by matching outlines of barrel hollows, section boundaries and grey/white matter transitions drawn from sections stained for cytochrome oxidase activity. New image planes, erected orthogonally on the tangential plane of the sections, were reconstructed computationally. The new planes represent  $20\ \mu\text{m}$  thick slices cut through a stack of 32 images.

#### Statistical analysis of rates of glucose utilization

The rate of glucose utilization for each cortical area of an animal is represented by the pixel-weighted average obtained from the autoradiograms of all sections cut through layer IV of barrel cortex. The mean rates for each cortical area, left and right, were tested for statistically significant differences between operated and unoperated mice with Student's *t*-tests (SAS®, SAS Institute, Cary, NC, USA). In both operated and unoperated mice side-to-side differences in each cortical area were tested with paired *t*-tests (SAS®). In all tests the null hypothesis was rejected for  $P \leq 0.05$ . For reasons we were unable to determine, glucose utilization rates of all areas of NOR.10 were more than two standard deviations higher than the respective group means, and the rates of NOR.03 and of LES.03 were more than two standard deviations lower than the group means. In spite of the differences in absolute rates, the patterns of stimulus-evoked tracer accumulation were similar to the patterns found in comparable experiments. Because of the quantitative discrepancies, however, we have excluded NOR.03, NOR.10 and LES.03 from the statistical analyses, which otherwise comprised all animals that had whiskers B1–3 and D1–3 stimulated throughout the whole duration of the deoxyglucose study.

#### Morphometry in barrel cortex

The radial thickness of layer IV of barrel cortex in the disorganized zone as well as in adjacent and distant barrels was determined by the number of sections stained for cytochrome oxidase activity in which these structures were identifiable as patches of high enzyme activity.

#### Histology of the whiskerpads

Whiskerpads from both sides of the snout were removed at the end of the deoxyglucose experiment and stored in 10% phosphate-buffered (pH 7.4) formalin. Two alternate series of  $20\ \mu\text{m}$ -thick sections were cut parallel to the surface of the skin in a cryostat at  $-22^\circ\text{C}$  and dried at room temperature. One series was stained with a modification of Liesegang's method (Cruz *et al.*, 1984), and when the differentiation of nerve fibres was poor the silver impregnation was repeated on the second series. If good quality was achieved, the other series was stained with Weil's haematoxylin method for myelin (Table 1).

#### Fibre counts in follicular nerves

Images of cross-sections of follicular nerves were digitized with a CCD camera mounted on a microscope (Ortholux II, Leitz, Wetzlar, FRG). The nerve fibres in each follicular nerve of whiskers B1–3, C1–4, D1–3 and whisker  $\gamma$  were counted with the image-processing software package IMAGE (W. Rasband, NIMH, USPHS, Bethesda, MD, USA).

## Results

#### Innervation of whisker follicles

Detailed descriptions of the morphology of the mouse whisker follicle have been provided by Dörfel (1985) and Rice *et al.* (1986). The site

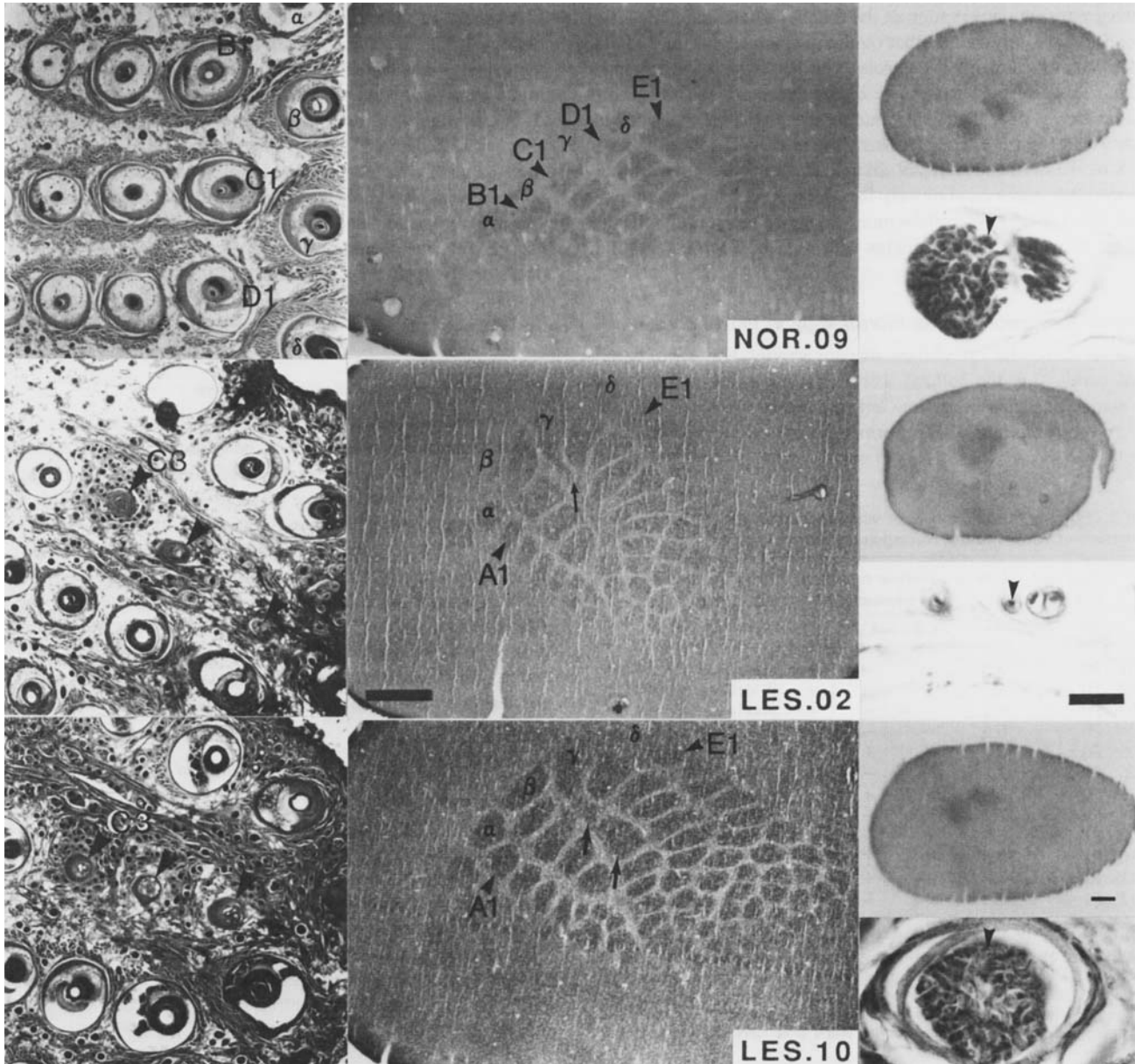


FIG. 1. The lesion in the whiskerpad and its impact on barrel cortex. Results from an unoperated control (NOR.09, top), and from mice which had the follicles of left whiskers C1, C2 and C3 removed on postnatal day 0 (LES.02, centre) and on postnatal day 1 (LES.10, bottom). Left column: micrographs of sections through the left whiskerpad stained by Liesegang's method (orientation: dorsal is up, rostral is left). Follicles are labelled in the top left micrograph. Follicular remnants developed at the site of the lesion (see arrowheads; the remnants at C3 are identified). Middle column: cytochrome oxidase activity in the right barrel cortex in sections cut tangentially to the surface of the pia. Barrel hollows, rich in cytochrome oxidase, are separated by bands of low enzyme activity in sides and septa. The barrels representing the straddlers  $\alpha$  to  $\delta$  and the posterior whisker in each row are labelled. Orientation: medial is up, rostral is right. Owing to the cutting angle the barrel of whisker A1 in NOR.09 cannot be seen in this section. In all sections, some barrels of the straddlers and whisker E1 stain faintly, because they are not fully cut. In the mice with lesion, the posterior barrels in rows B and D and barrel  $\gamma$  are enlarged. Arrows point to segments of high staining intensity, which cannot be attributed to any barrel. The bar in the centre panel pertains to the panels in the left and in the middle column and represents 500  $\mu\text{m}$ . Right column: the upper panels show autoradiograms of the [ $^{14}\text{C}$ ]deoxyglucose distribution in the section (NOR.09) or in sections adjacent to those shown in the middle column. Left whiskers B1–3 and D1–3 were stimulated during the deoxyglucose procedure. Tracer accumulation is proportional to grain density. Orientation: medial is up, rostral is right; the bar near the bottom of the autoradiogram represents 500  $\mu\text{m}$ . The lower panels show the deep follicular nerve of whisker C4 as seen in Liesegang preparations used for counting nerve fibres. Note that the follicle in LES.02 received only four fibres. Single fibres are indicated by arrowheads (posterior is up, ventral is right; the bar at LES.02 represents 20  $\mu\text{m}$ ).

of the lesion and its surrounding whisker follicles are shown in Figure 1 (left column). In eight mice (indicated in Table 2), follicle-like remnants (marked with arrowheads in Fig. 1), some bearing a minute hair, remained at the site of the lesion. In three cases the remnants

were innervated by a deep follicular nerve (indicated in Table 2). In Table 3, the number of fibres in the deep follicular nerves of operated mice are grouped by the two morphological types of altered barrel cortex encountered, i.e. a disorganized zone with poorly defined barrels

and an ill-defined barrel-like disorganized zone (see next section). In the two groups, the innervation of the follicles surrounding the lesion was considerably lower than that on the unoperated side and in both whiskerpads of unoperated controls. The loss was highest in mice featuring an ill-defined barrel-like disorganized zone. Examples of follicular nerves near their entry into the deep portion of the follicle are shown in Figure 1 (right column, lower panels) for whisker C4 of LES.02, LES.10 and NOR.09. In LES.02 that follicle, though fully developed, was innervated by only four nerve fibres as opposed to the normal 105 (Table 3). Superficial innervation was found in all follicular remnants as well as in the follicles with reduced deep innervation.

### Effects of the lesion on the morphology in barrel cortex

In sections stained for cytochrome oxidase activity, hollows of barrels stained darkly (i.e. the hollows were high in enzyme activity), and were distinctly separated by low enzyme activity in sides and septa (Fig. 1, centre column). The normal pattern of barrel hollows in

tangential sections through layer IV is shown in Figure 1 (right hemisphere of unoperated control NOR.09). The pattern of barrel hollows in the left barrel cortex of operated mice, i.e. ipsilateral to the lesion, was identical to that in unoperated controls. In contrast, in the barrel cortex contralateral to the lesion, the hollows of barrel  $\beta$ , barrel  $\gamma$  and the posterior barrels in rows B and D were enlarged (Fig. 1, LES.02 and LES.10). The enlarged barrels surrounded the 'disorganized zone', a zone as rich in cytochrome oxidase as barrel hollows, which was not clearly associated with any barrel. Its location was homeotopic to that of posterior barrels in row C in normal barrel cortex. The size of barrels anterior in row C, i.e. barrel C4 and up, occasionally appeared diminished (LES.02 in Figs 1 and 2) or else normal. Using the characterization of Jeanmonod *et al.* (1981), we distinguished the following two types of morphological patterns.

### Ill-defined barrel-like disorganized zone

In the Nissl-stained preparations five mice had no sides and septa abutting the disorganized zone at the border with barrel  $\gamma$  and barrels in row D (LES.02 in Fig. 2). In preparations stained for cytochrome oxidase activity the hollows of these barrels were fused with the disorganized zone (LES.02 in Fig. 1; LES.01, LES.04, LES.06 and LES.07 in Fig. 3). The zone was subdivided by lines of cell bodies. In all mice barrel  $\beta$  and the barrels in row B were clearly separated from the disorganized zone by a band of low enzyme activity. Hollows of barrels were often fused, however, in row B, and there was no clear boundary between the disorganized zone and barrel C4. An ill-defined barrel-like disorganized zone occurred only in animals subjected to the lesion on postnatal day 0 (Table 2).

### Poorly defined barrels in the disorganized zone

In Nissl-stained preparations seven mice had sides and septa between the disorganized zone and barrel  $\gamma$ , barrel C4, and barrels in row D (LES.10 in Fig. 2). Sides and septa were also found between the barrels in rows B and D. Furthermore, sides and septa had developed in the disorganized zone, forming two or three compartments. In sections stained for cytochrome oxidase activity, these compartments were separated by narrow strips of low enzyme activity (compare LES.10 in Figs 1 and 2). The anterior compartment had enlarged. Low enzyme activity separated the disorganized zone from all neighbouring barrels (distinctly visible in LES.10 in Fig. 1 and LES.09 in Fig. 3). Poorly

TABLE 2. Efficacy of the removal of whisker follicles and its effects on the development of barrels in the corresponding barrel cortex

Code	Postnatal day	Hour of lesion	Follicle remnants in whiskerpad at			Morphological type of barrel cortex
			C1	C2	C3	
LES.01	P0	5.5	-	-	-	ill-defined barrel-like
LES.02	P0	5.7	+	+	+	ill-defined barrel-like
LES.03	P0	6	-	+	+*	poorly defined barrels
LES.04	P0	6.3	-	-	-	ill-defined barrel-like
LES.05	P0	6.7	+	+	+	poorly defined barrels
LES.06	P0	6.8	-	-	-	ill-defined barrel-like
LES.07	P0	7	-	+	+	ill-defined barrel-like
LES.08	P0	7.2	+	-	-	poorly defined barrels
LES.09	P1	30.3	+	-	+*	poorly defined barrels
LES.10	P1	30.5	+	+	+	poorly defined barrels
LES.11	P1	30.7	+	+	+	poorly defined barrels
LES.12	P1	30.8	+*	+	+	poorly defined barrels

Whisker follicles C1, C2 and C3 were surgically removed from the left side of the snout of newborn mice. The experiments are listed by the postnatal day (P0 is the day following the detection of a litter) and the hour after detection of the litter, at which the follicles were removed. The efficacy of the intervention in the whiskerpad, i.e. presence (+) or absence (-) of follicular remnants and whether they were innervated (\*), and the resulting barrel pattern in the cortex contralateral to the lesion were investigated at adulthood.

TABLE 3. Effects of neonatal removal of whisker follicles on the number of nerve fibres (mean  $\pm$  SD) innervating neighbouring whisker follicles

Group	Type of barrel cortex	Number of nerve fibres per follicular nerve at whisker (mean $\pm$ SD)										
		$\gamma$	B1	B2	B3	C1 <sup>a</sup>	C2 <sup>a</sup>	C3 <sup>a</sup>	C4	D1	D2	D3
LES (n = 5)	ill-defined barrel-like	left whiskerpad (with lesion)										
		148 $\pm$ 5	144 $\pm$ 5	86 $\pm$ 72	60 $\pm$ 73	0 <sup>a</sup>	0 <sup>a</sup>	0 <sup>a</sup>	17 $\pm$ 23	144 $\pm$ 4	135 $\pm$ 3	122 $\pm$ 8
LES (n = 7)	poorly defined barrels	right whiskerpad										
		152 $\pm$ 4	144 $\pm$ 1	143 $\pm$ 2	136 $\pm$ 8	146 $\pm$ 4	136 $\pm$ 4	134 $\pm$ 3	101 $\pm$ 3	145 $\pm$ 3	140 $\pm$ 4	133 $\pm$ 4
LES (n = 7)	poorly defined barrels	left whiskerpad (with lesion)										
		154 $\pm$ 14	141 $\pm$ 12	146 $\pm$ 4	137 $\pm$ 8	12 $\pm$ 31 <sup>a</sup>	0 <sup>a</sup>	22 $\pm$ 38 <sup>a</sup>	104 $\pm$ 6	146 $\pm$ 6	117 $\pm$ 50	130 $\pm$ 3
NOR (n = 11)	normal	right whiskerpad										
		156 $\pm$ 4	145 $\pm$ 5	145 $\pm$ 3	142 $\pm$ 4	149 $\pm$ 6	139 $\pm$ 3	129 $\pm$ 6	106 $\pm$ 7	145 $\pm$ 4	141 $\pm$ 5	130 $\pm$ 2
NOR (n = 11)	normal	left and right whiskerpads										
		154 $\pm$ 8	148 $\pm$ 8	144 $\pm$ 4	139 $\pm$ 4	152 $\pm$ 6	141 $\pm$ 3	132 $\pm$ 4	109 $\pm$ 5	146 $\pm$ 3	136 $\pm$ 4	133 $\pm$ 3

<sup>a</sup>Removed whisker follicles.

<sup>b</sup>Means  $\pm$  SD of summed fibre counts of the follicles examined in each whiskerpad. The total innervation in the whiskerpads with lesion is statistically significantly smaller than that of the unoperated whiskerpads (*t*-test,  $P \leq 0.05$ ).

defined barrels were found in all mice subjected to the lesion on postnatal day 1 and three mice subjected to the lesion on postnatal day 0 (Table 2).

Sections stained for cytochrome oxidase activity showed that in barrel cortex of operated mice the intensely stained band of patches indicative of layer IV was thinner in the deprived territory than in normal barrel

cortex. High cytochrome oxidase activity in the disorganized zone and in the adjacent portion of enlarged barrels extended radially between 80 and 180  $\mu\text{m}$  (the median was 120  $\mu\text{m}$ ), whereas in the portion of enlarged barrels near rows A and E high enzyme activity spanned on average 220  $\mu\text{m}$ . This thickness was similar to that of the hollows of normal barrels in rows B, C and D.

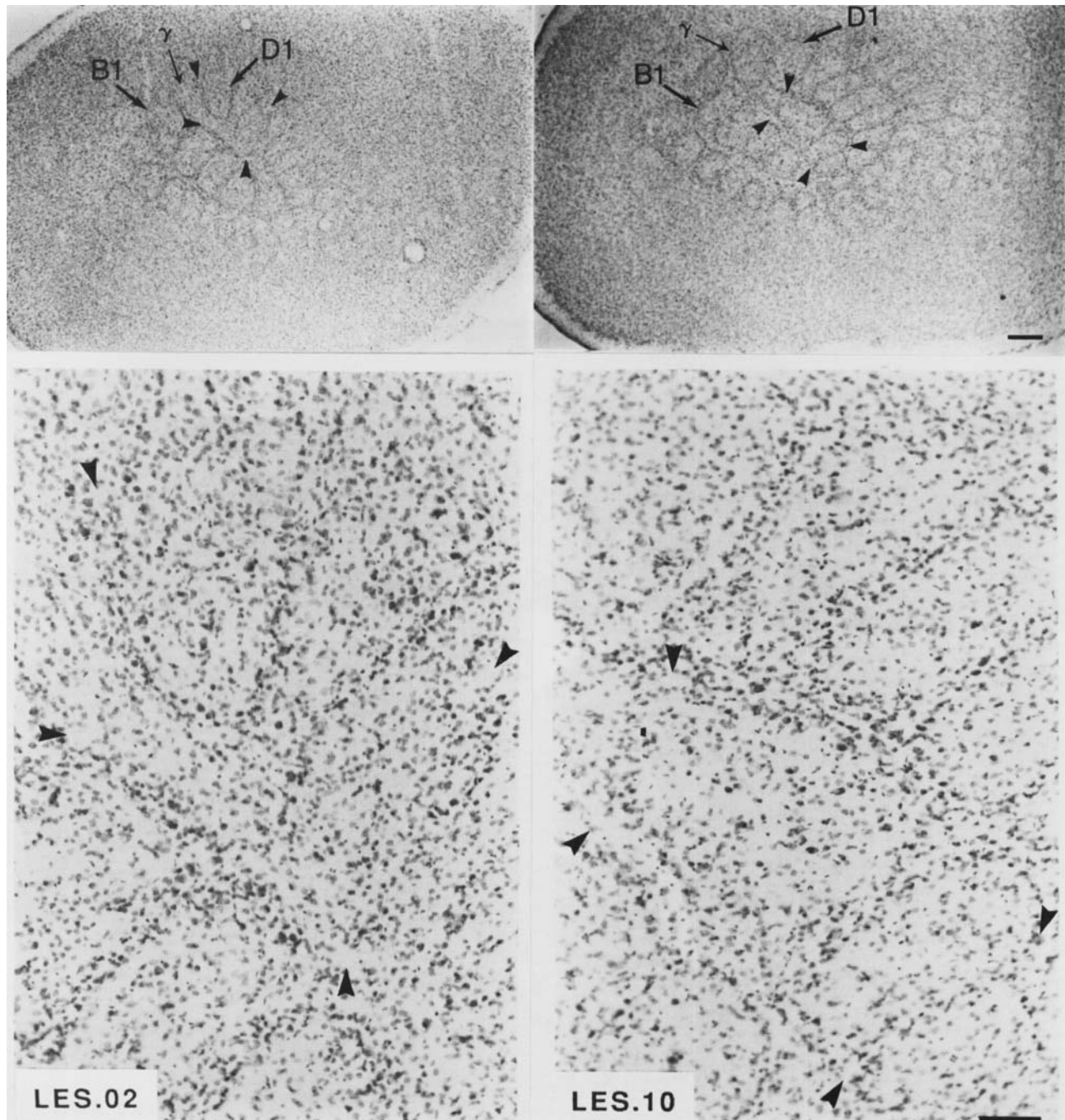


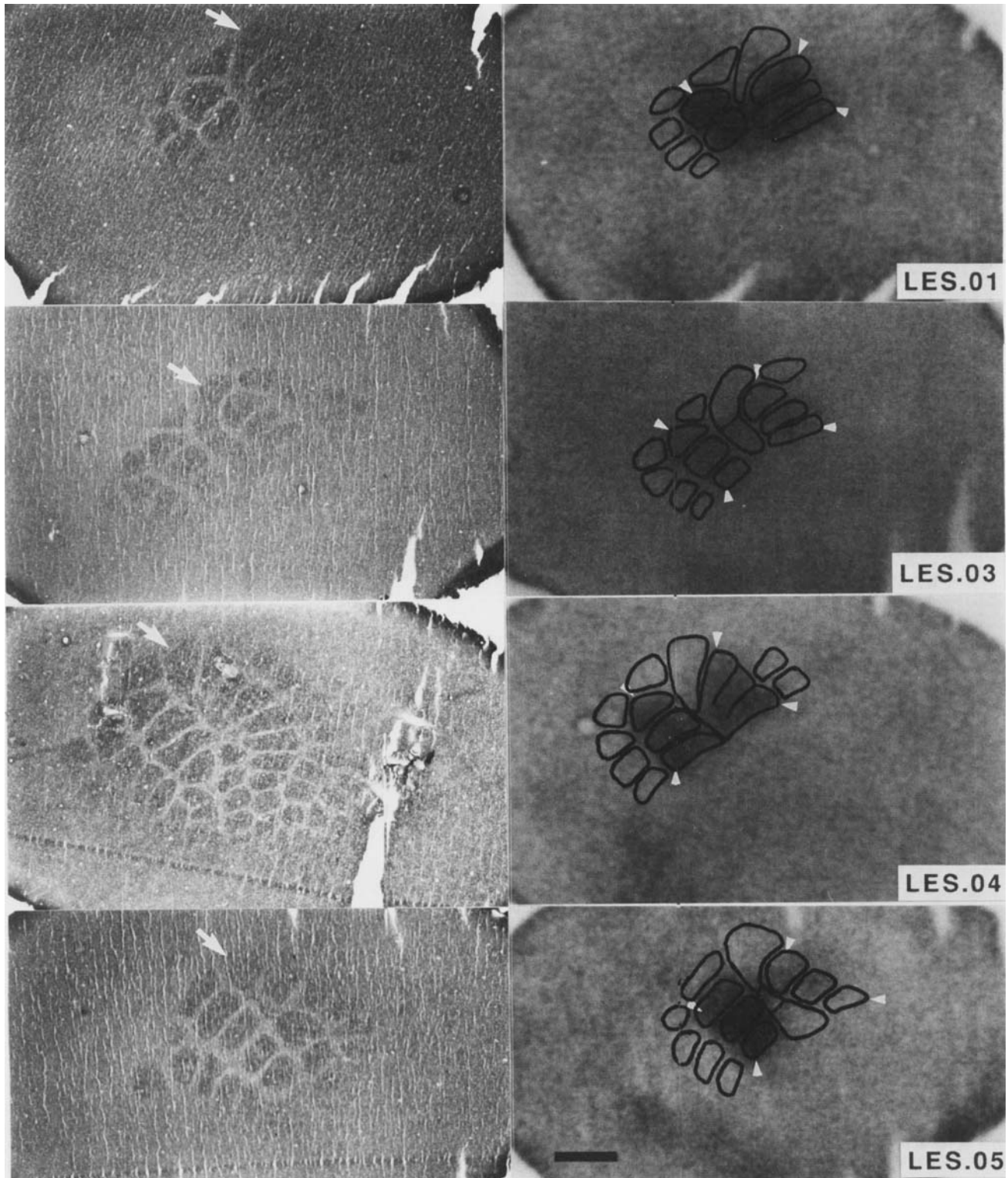
FIG. 2. Cytoarchitecture of altered barrel cortex. Micrographs of sections cut tangentially through the right hemisphere and stained for Nissl substance. In layer IV, two types of cytoarchitecture can be distinguished: an ill-defined barrel-like structure (LES.02; left column) and poorly defined barrels (LES.10; right column). Micrographs in the bottom row are partial enlargements of those in the top row. Identical areas are marked with arrowheads, and barrels B1, D1 and  $\gamma$  are marked in the top row of panels. Orientation: medial is up, rostral is right. The bar in the top right micrograph represents 500  $\mu\text{m}$ ; the bar in the bottom right micrograph represents 50  $\mu\text{m}$ .

*Effects of the lesion on stimulus-evoked metabolic responses in barrel cortex*

*Patterns of deoxyglucose accumulation*

Whisker stimulation had no effect on tracer accumulation in the ipsilateral barrel cortex of either unoperated or operated mice. In the

contralateral barrel cortex, however, stimulation of whiskers B1–3 and D1–3 increased tracer accumulation markedly in two prominent, but discrete areas in unoperated controls (NOR.09 in Fig. 1, right column, upper panel). In operated mice we found only one area of markedly increase tracer accumulation (Figs 1 and 3, right column). Superimposing the patches of high cytochrome oxidase activity on



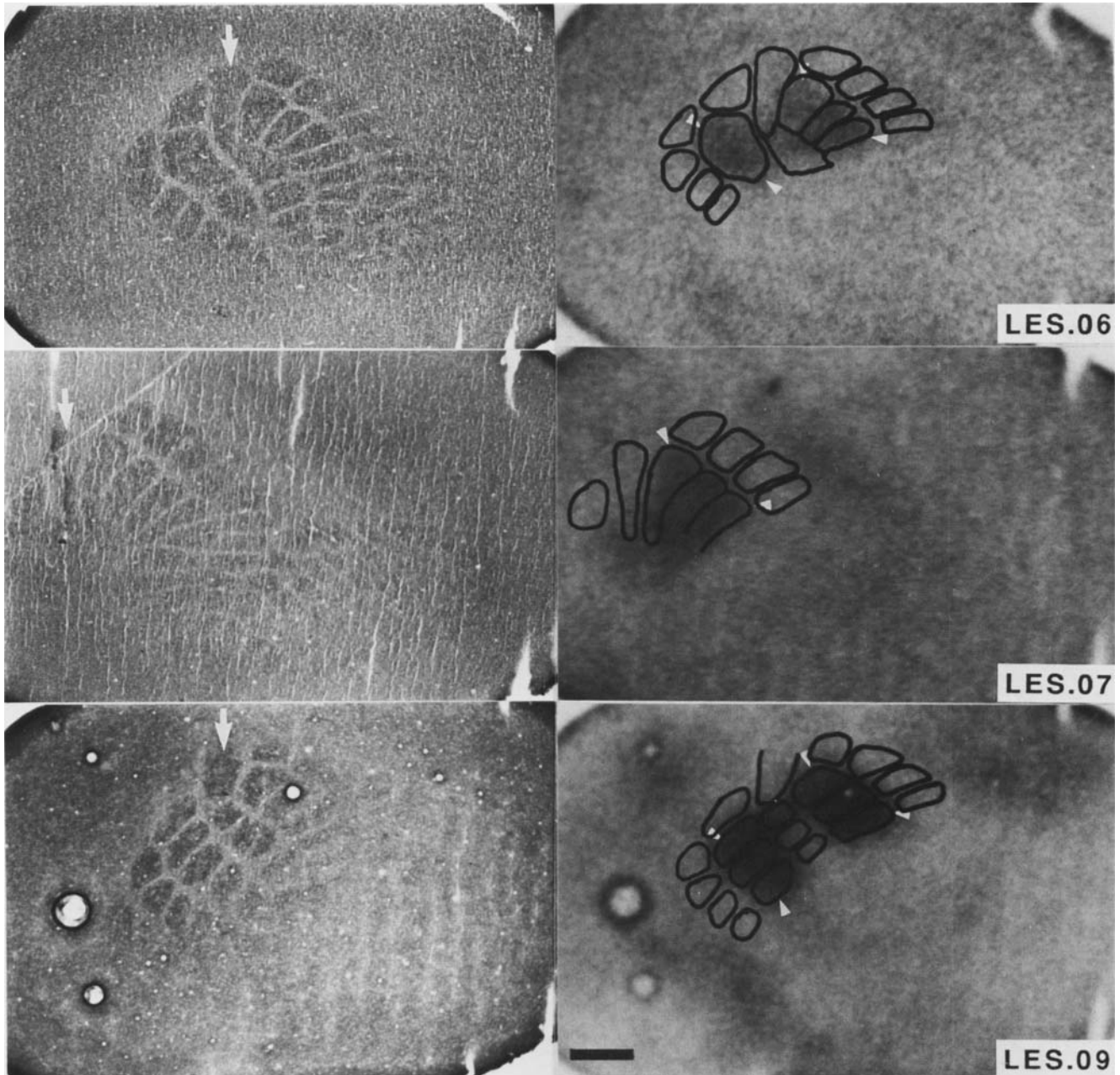


FIG. 3. Patterns of deoxyglucose accumulation in barrel cortex of mice with lesion: effect of the time of follicle removal. Tangential sections stained for cytochrome oxidase activity showing the barrel pattern (left column of panels) and autoradiograms showing the pattern of [ $^{14}\text{C}$ ]deoxyglucose accumulation from the adjacent section or, in LES.09, from the same section (right column). The outlines of the patches of high cytochrome oxidase activity in the disorganized zone and the hollows of barrels neighbouring the zone are shown in the overlays. Left whiskers B1–3 and D1–3 were stimulated during the deoxyglucose procedure. Starting at the top, the experiments are ordered in sequence of increasing time of lesion (for LES.02 and LES.10 see Fig. 1). The arrows point to barrel  $\gamma$ . Arrowheads mark the caudal limits of barrels B1 and D1 and the rostral limits of barrels B3 and D3. In LES.06, the barrels in row B were not separable. In LES.01 barrel B3 and in LES.07 barrels B1 and B3 appeared in neighbouring sections. In all cases whisker stimulation increased tracer accumulation in the corresponding enlarged barrels and in the disorganized zone intercalated between them. LES.05 had lost whisker D3 shortly after stimulation had begun. Tracer accumulation in this barrel is not increased. Orientation: medial is up, rostral is right. The bars in the left lower corner of the right panels for LES.05 and LES.09 represent 500  $\mu\text{m}$  and hold for all panels.

corresponding autoradiograms showed that in unoperated controls the two areas of high tracer accumulation colocalized with barrels B1–3 and D1–3 (NOR.09 in Fig. 4). In operated mice the area of markedly increased tracer accumulation covered enlarged barrels B1–3 and D1–3 and the disorganized zone (Fig. 3 and, for LES.02 and LES.10, Fig. 4). Reduced follicular innervation did not prevent increases in

tracer accumulation in the corresponding barrels (in Fig. 3: barrel B2 in LES.01; barrel D2 in LES.05; barrels B2 and B3 in LES.06). In mice with an ill-defined barrel-like disorganized zone, tracer accumulation was increased in the whole zone, whereas in mice with poorly defined barrels tracer accumulation was increased only in its posterior compartments (LES.03 and LES.09 in Fig. 3 and LES.10 in Fig. 4).

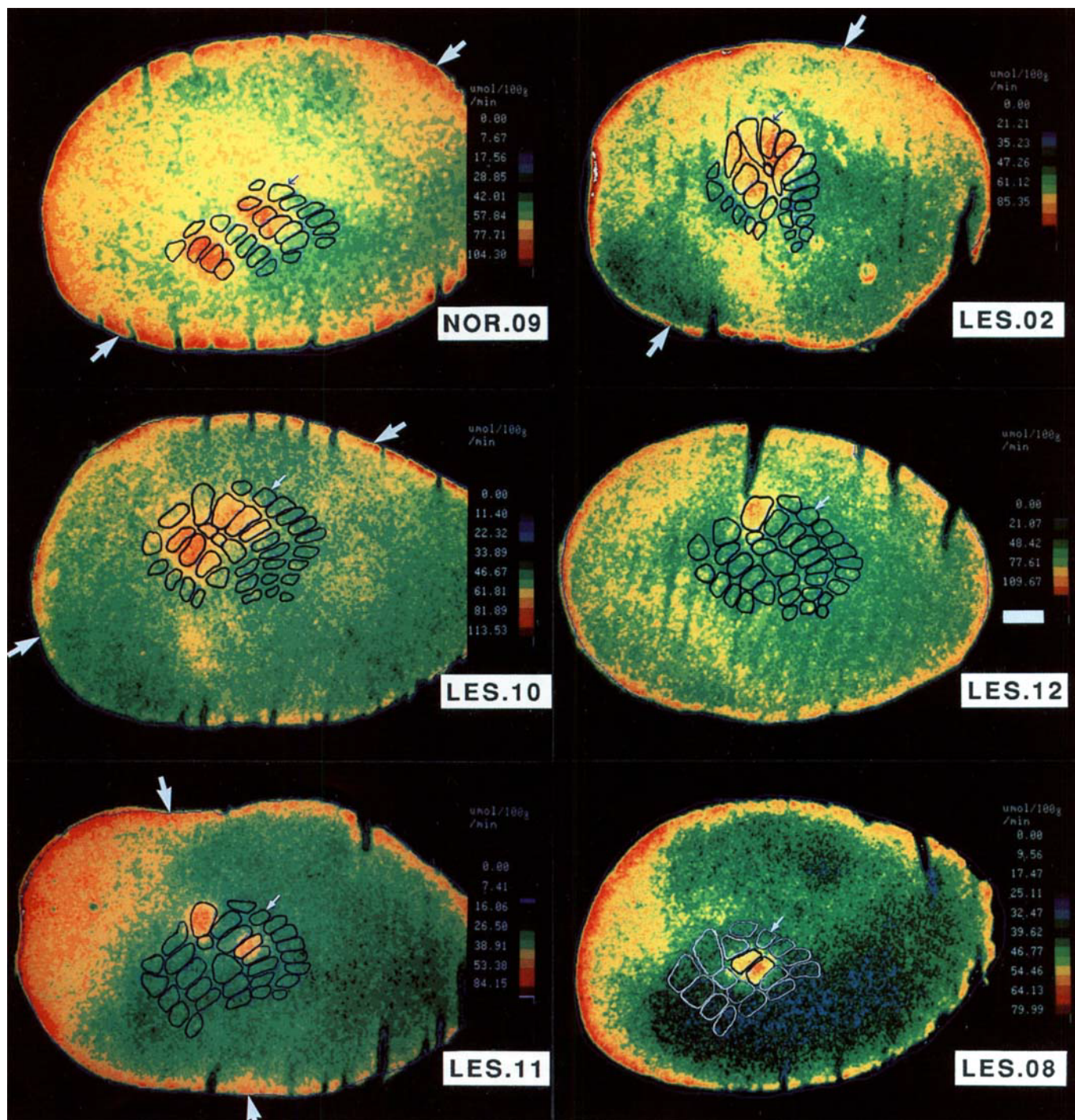


FIG. 4. Local rates of glucose utilization in barrel cortex. Pseudocolour images of rates of glucose utilization digitized from autoradiograms of tangential sections through the right cortical hemisphere (the rates are indicated by the colour bar on the right of each autoradiogram). Images are shown from three mice which had left whiskers B1–3 and D1–3 stimulated during the deoxyglucose procedure: an unoperated control (NOR.09), an operated mouse with ill-defined barrel-like structures in barrel cortex (LES.02) and an operated mouse with poorly defined barrels (LES.10). In addition, images are shown from operated mice with poorly defined barrels which had left whisker  $\gamma$  (LES.12), left whiskers  $\gamma$  and D3 (LES.11) and left whiskers D2 and D3 (LES.08) stimulated. Superimposed on the images are the outlines of patches of high cytochrome oxidase activity in the disorganized zone and the hollows of surrounding barrels, visible in the corresponding sections or in directly adjacent sections (for NOR.09, LES.02 and LES.10 see Fig. 1). The small arrows point to barrel E1 and, in LES.02, to barrel D1. The large arrows at image boundaries indicate the points between which the images in Figure 5 were reconstructed. Orientation: medial is up, rostral is right. The white bar at the right of the image of LES.12 represents 500  $\mu\text{m}$  and holds for all panels.

All operated mice, except LES.04 and LES.09, had increased tracer accumulation in barrel  $\gamma$  near the disorganized zone (Figs 3 and 4). Since the mice with an ill-defined barrel-like disorganized zone had

whisker follicles removed on postnatal day 0 (Table 2), early lesions were apparently associated with the most comprehensive increase in deoxyglucose accumulation in the territory deprived by the lesion.

TABLE 4. Effects of stimulation of left whiskers B1–3 and D1–3 on rates of glucose utilization in the barrel cortex (mol/100 g/min)

Group	Side	Area in barrel cortex				
		A1–3	B1–3	C1–3	D1–3	E1–3
NOR	left	55 ± 3	56 ± 3	58 ± 3	57 ± 3	58 ± 3
	right	62 ± 3	94 ± 4 <sup>a</sup>	64 ± 3	83 ± 4 <sup>a</sup>	62 ± 3
LES	left	56 ± 3	57 ± 3	57 ± 3	58 ± 3	58 ± 3
	right	62 ± 1	88 ± 2 <sup>a</sup>	85 ± 3	87 ± 3 <sup>a</sup>	63 ± 3

Means and SEM for unoperated controls (NOR;  $n = 11$ ) and mice with lesion (LES;  $n = 7$ ). NOR.03, NOR.10 and LES.03 were excluded because they had exceptionally high or low rates (see Materials and methods).

<sup>a</sup>Barrels representing stimulated whiskers.

TABLE 5. Effects of whisker stimulation on rates of glucose utilization in anterior and posterior compartments of the disorganized zone in barrel cortex of mice in which neonatal removal of whisker follicles led to poorly defined barrels

Code	Stimulated whiskers	Rate of glucose utilization ( $\mu\text{mol}/100 \text{ g}/\text{min}$ )		Difference (%)
		posterior compartment(s)	anterior compartment	
LES.03	B1–3 and D1–3	54	43	26
LES.09	B1–3 and D1–3	79	56	41
LES.10	B1–3 and D1–3	77	56	38
LES.08	D2 and D3	42	38	11
LES.11	$\gamma$ and D3	38	29	31
LES.12	$\gamma$	52	45	16

### Regional rates of glucose utilization

Quantification of the rates of glucose utilization corroborated and extended the qualitative observations described above. In unoperated controls, rates of glucose utilization in barrels A1–3, B1–3, C1–3, D1–3 and E1–3 contralateral to stimulation were higher than the rates in the homeotopic areas ipsilateral to stimulation (Table 4). In agreement with the qualitative observations, the increase was highest in barrels B1–3 and D1–3, i.e. the barrels representing the stimulated whiskers (on average 73 and 48% respectively). In contrast, the rates in barrels A1–3, C1–3 and E1–3 were increased only between 8 and 15%. Side-to-side differences of all areas except barrels E1–3 were statistically significant in paired Student's *t*-tests. In operated mice, rates of glucose utilization in the five assessed areas of barrel cortex contralateral to stimulation were statistically significantly higher ( $P \leq 0.05$ ; paired Student's *t*-tests) than those in the homeotopic areas of ipsilateral barrel cortex (Table 4). The increase in rates was on average 12% in barrels A1–3 and E1–3 and 56 and 54% in barrels B1–3 and D1–3 respectively. We took the rates of glucose utilization of the disorganized zone in mice with poorly defined barrels to be represented exclusively by the rates in the posterior compartments of the zone because it was only there that metabolic responses to stimulation were found. In the anterior compartment rates of glucose utilization remained close to control values (Table 5). In contrast to the small side-to-side difference in rates of glucose utilization in barrels C1–3 of unoperated mice (on average 12%), the rates in the disorganized zone of operated mice were 50% higher than those in barrels C1–3 of the unstimulated hemisphere. The increase was 30% in comparison with the rates of glucose utilization found in barrels C1–3 on the stimulated hemisphere of unoperated controls. In the area-to-area comparison of rates of operated and unoperated mice, this was the only one with a statistically significant difference ( $P \leq 0.05$ ).

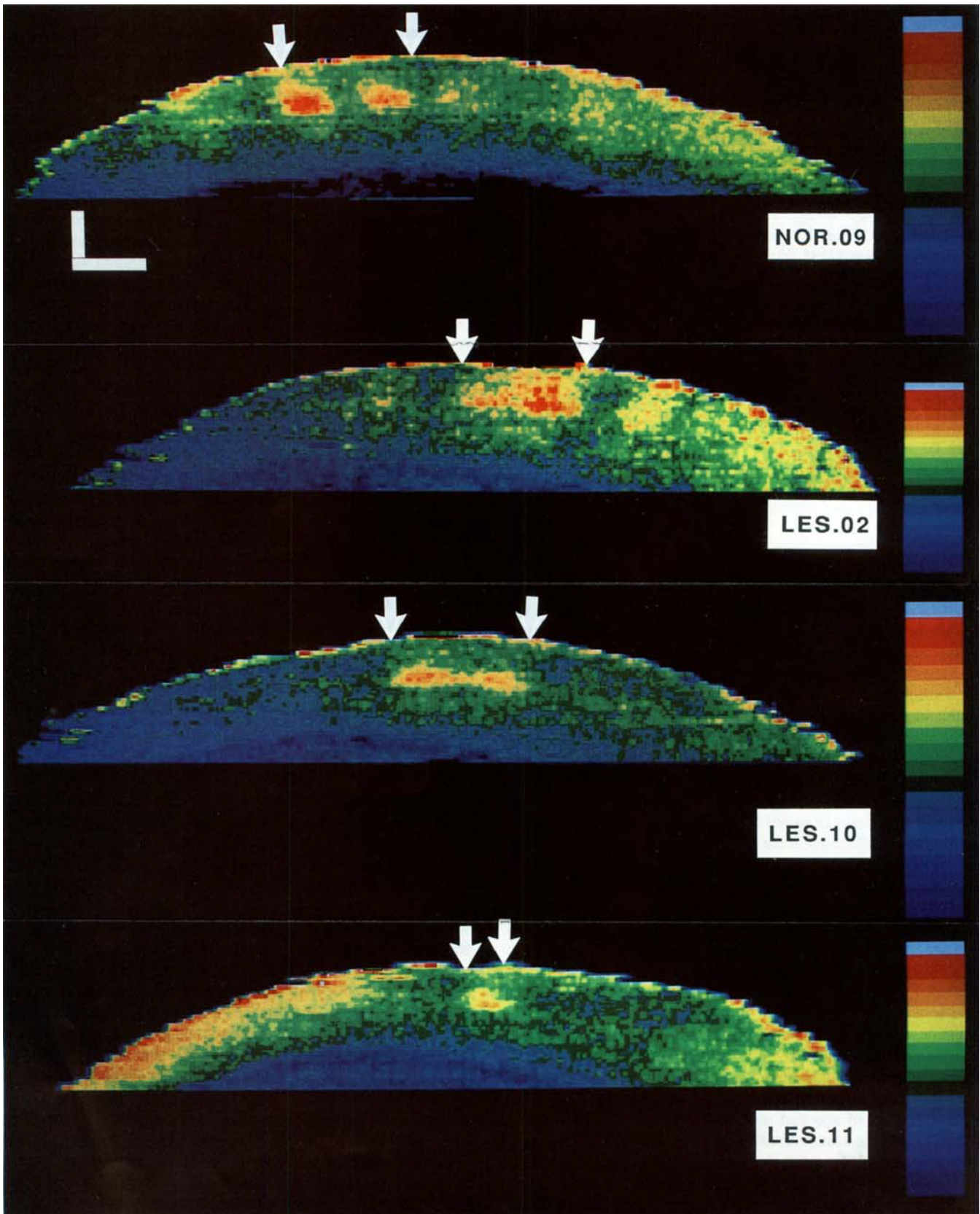
The three operated mice which had whisker  $\gamma$  (LES.12), whiskers  $\gamma$  and D3 (LES.11), and whiskers D2 and D3 (LES.08) stimulated, all had poorly defined barrels. The greatest increase in rates of glucose utilization occurred in the barrels representing the stimulated whiskers (Fig. 4). Quantification further revealed that in the three mice rates of glucose utilization in the posterior compartment(s) of the disorganized zone were increased over the rates in its anterior compartment (Table 5). The difference was 11% with the stimulation of whisker D2 and D3, 16% with the stimulation of whisker  $\gamma$ , and 31% with the stimulation of whiskers  $\gamma$  and D3. In contrast, the difference obtained with the stimulation of six whiskers in mice with poorly defined barrels was on average 37% (Table 5).

### Three-dimensional reconstruction of the metabolic responses

Three-dimensional reconstructions of the activation pattern showed that in unoperated controls as well as in all operated mice the highest rates of glucose utilization evoked by whisker stimulation were located in cortical layer IV. Lesser increases in metabolism radiated into layer I and layer VI (Fig. 5). In controls stimulation of whiskers B1–3 and D1–3 resulted in two metabolic columns through barrel rows B and D, separated by an inactive barrel column in row C (NOR.09, Fig. 5). In operated mice exposed to the same stimulus, there was no gap between row B and row D; increases in metabolic activity in the enlarged barrels and in the disorganized zone blended together (LES.02 and LES.10, Fig. 5). Analogous to the metabolic columns protruding through normal and enlarged barrels, rates of glucose utilization in the disorganized zone were highest in layer IV and less increased in supra- and infragranular layers. In harmony with the observed thinning of layer IV in sections stained for cytochrome oxidase activity, the radial extent of the focus of activation in the disorganized zone and in the adjacent portion of the enlarged barrels was smaller than that in the portion of the enlarged barrels near rows A and E (markedly visible in LES.10). Similarly, in LES.11 (Fig. 5) the band of highest rates of glucose utilization was thicker in the caudal portion of barrel  $\gamma$  than in its rostral portion. The rostral portion is the actual site of enlargement towards the disorganized zone. Analogous to metabolic columns across normal barrels, rates of glucose utilization were slightly increased in supra- and infragranular layers above and below barrel  $\gamma$ .

### Discussion

The present study investigates plasticity of the functional whisker map in mouse barrel cortex as a consequence of the removal of whisker follicles shortly after birth. Its major findings are summarized in Figure 6, in which the patterns of activation in response to stimulation of whiskers B1–3 and D1–3 are superimposed on the structure of barrel cortex. In unoperated mice the highest metabolic responses to the stimulation of whiskers B1–3 and D1–3 are restricted to the appropriate barrels, i.e. barrels B1–3 and D1–3, in barrel cortex contralateral to stimulation. Only small increases in rates of glucose utilization are found in adjacent inappropriate barrels (Fig. 6, top schema). In contrast, in mice with lesions, the deprived territory of barrel cortex became metabolically as responsive to the stimulation of whiskers B1–3 and D1–3 as the appropriate barrels of the stimulated whiskers. We distinguished two morphological types of altered barrel cortex, each associated with a specific pattern of metabolic responses. In barrel cortex with an ill-defined barrel-like territory, the area responding to the stimulus comprised the barrels corresponding to the stimulated whiskers, which were enlarged, the whole disorganized zone and barrel  $\gamma$ , partially in the majority of cases, or entirely in LES.02 (Fig. 6, centre schema). In barrel cortex with poorly defined barrels, the metabolically activated area spared most of barrel  $\gamma$  and the anterior



part of the disorganized zone (Fig. 6, bottom schema). Therefore, in these cases the area activated by whisker stimulation was smaller than in mice with an ill-defined barrel-like territory.

#### *Metabolic maps in normal neocortex*

The present study confirms recent reports (Durham and Woolsey, 1977; Melzer *et al.*, 1985; Chmielowska *et al.*, 1986) that the map of metabolic responsiveness to whisker stimulation in normal mouse barrel cortex indeed concurs with the morphological whisker map in layer IV. This finding agrees with the observation of single- and multi-unit recordings on barrel cortex of anaesthetized rats (Welker, 1971; Armstrong-James, 1975; Simons, 1978, 1985; Chapin and Lin, 1984; Ito, 1985) and mice (Nussbaumer and Van der Loos, 1985) that neurons in layer IV respond most vigorously to the stimulation of their appropriate whisker, i.e. the whisker represented by the barrel in which the recorded neurons are located. Our finding disagrees, however, with reports that such neurons may respond to deflection of surrounding whiskers almost as vigorously, though dependent on the level and type of anaesthesia (Armstrong-James, 1975; Chapin and Lin, 1984; Nussbaumer and Van der Loos, 1985; Armstrong-James and Fox, 1987). The increased rates of glucose utilization in barrel hollows may stem from neural spiking activity, pre- and/or postsynaptically, at the endings of afferents originating in the main thalamic relay for somatosensory input, i.e. the barreloids in the ventrobasal nucleus (Van der Loos, 1976). Their terminations in layer IV fill barrel hollows completely, sparing sides and septa (Lorente de N6, 1922; Killackey, 1973; for a view on a tangential section see Killackey and Leshin, 1975), and distribute in a pattern congruent with that of cytochrome oxidase activity (Wong-Riley and Welt, 1980).

Hand (1981) was the first to demonstrate that with the stimulation of one whisker rates of glucose utilization in barrel cortex not only increase in the granular layer, but also in the supra- and infragranular layers, forming a column of metabolic activation. Since thalamocortical afferents originating in the ventrobasal nucleus terminate only in layers III and IV and at the transition of layers V and VI (Bernardo and Woolsey, 1987; Jensen and Killackey, 1987), the columnar activation, comprising all cortical layers, indicates that intrinsic cortical connections were activated (Chapin *et al.*, 1987; White and Keller, 1987; Keller and White, 1987; Elhanany and White, 1990; Bernardo *et al.*, 1990a,b). The activation of neural connections between barrels (Bernardo *et al.*, 1990a,b) may be the cause of the slight increase in rates of glucose utilization in inappropriate barrels A1–3 and C1–3. Indeed, Armstrong-James *et al.* (1991) provide evidence from single-unit recordings in rat barrel cortex that the neural activation in response to the stimulation of whiskers neighbouring the appropriate whisker depends on functional barrels adjacent to the appropriate barrel.

The interpretation that changes in rates of glucose utilization reflect neural spiking activity in fields of termination is supported by the observation that electrical stimulation of the rat sciatic nerve, which evokes spiking activity in its nerve fibres, increases the rates of glucose utilization linearly with spike frequency only in the dorsal horn of the

spinal cord, where most sciatic nerve afferents terminate, and not in the cell bodies in the dorsal root ganglion (Kadekaro *et al.*, 1985). Therefore, it may not be surprising that maps of metabolic activation in layer IV of barrel cortex obtained with the deoxyglucose method and those derived from electrophysiological recordings are compatible only when in electrophysiological recordings neural responses of highest probability (one spike per stimulus and up) and shortest latency (shorter than 11 ms), i.e. responses of neurons directly receiving input from the ventrobasal nucleus, are considered (Armstrong-James and Fox, 1987). We hypothesize that the topological metabolic representation of whisker follicles in barrel cortex is constituted by thalamocortical inputs providing the primary 'landscape' on which final features are sculpted by intracortical circuitry and, probably, cortico-subcortical feedback loops (Sessle and Dubner, 1971; Dubner and Sessle, 1971; Simons, 1985; Simons and Carvell, 1989; Armstrong-James and Callahan, 1991; Armstrong-James *et al.*, 1991; Welker *et al.*, 1992).

#### *Metabolic maps in altered neocortex*

In the present study whisker follicles were removed ~2 days before barrels emerge (Rice and Van der Loos, 1977), but when the endings of thalamocortical afferents originating in the ventrobasal nucleus have already become separated into clusters (Senft and Woolsey, 1991) surrounded by envelopes featuring glial fibrillary acidic protein-positive glia and lectin-binding glycoconjugates (Steindler *et al.*, 1990). The intervention obviously affected the segregation of fields of termination into discrete whisker-specific morphological and functional entities in the deprived territory. In place of normal barrels, enlarged 'barrels' developed surrounding a disorganized zone. In five mice sides and septa abutting the disorganized zone were disrupted and hollows of enlarged barrels were fused with the zone. In spite of the structural changes, the 'barrels' adjacent to the disorganized zone could be delineated based on remaining sides and septa and on the patches rich in cytochrome oxidase. Each of these incomplete barrels could be assigned a whisker according to the barrel's location in the topological map. Even a drastic reduction in follicular innervation did not prevent metabolic responses to whisker stimulation in such barrels.

#### *Stimulus-related activation of enlarged barrels*

Whisker stimulation markedly increased rates of glucose utilization in the appropriate barrels, filling their entire enlarged cross-section. Inasmuch as the metabolic activation spanned radially all cortical layers, it would appear that functional intracortical circuitry had also developed in enlarged barrels. Interestingly, enlarged barrels may not be exclusively responsive to the deflection of their appropriate whiskers. Barrel  $\gamma$  could be activated with the stimulation of whiskers B1–3 and D1–3. Though the magnitude and the spatial spread of the activation varied, this finding indicates the possibility of a loss in whisker specificity of neural responses in enlarged barrels.

#### *Stimulus-related activation in the disorganized zone*

Stimulation of whiskers adjacent to the lesion did not only activate the corresponding enlarged barrels, but also the disorganized zone. In all

FIG. 5. Radial distribution of stimulus-evoked metabolic responses through the cortical thickness. Pseudocolour-coded images of rates of glucose utilization (red, high; blue, low) in a plane orthogonal to the tangential sections through the right cortical hemisphere. The endpoints of the lines of slicing are indicated in Figure 4. The images represent an unoperated control (NOR.09), a mouse in which removal of whisker follicles resulted in ill-defined barrel-like structures (LES.02), and two mice in which this lesion resulted in poorly defined barrels (LES.10 and LES.11). LES.11 had left whiskers  $\gamma$  and D3 and the other three mice had left whiskers B1–3 and D1–3 stimulated during the deoxyglucose procedure. The images were computationally reconstructed from autoradiograms (see Materials and methods). In NOR.09, LES.02 and LES.10, arrows at the pia point to the borders between rows A and B (left) and rows D and E (right). The discrepancy in location of the barrels among the three mice is the result of different cutting planes. In LES.11 arrows point to the caudal (left) and the rostral (right) border of barrel  $\gamma$ . Orientation: dorsal is up, lateral is left. The compass for the four panels is shown in the top panel. Its vertical bar represents 500  $\mu\text{m}$  and its horizontal bar represents 300  $\mu\text{m}$ .

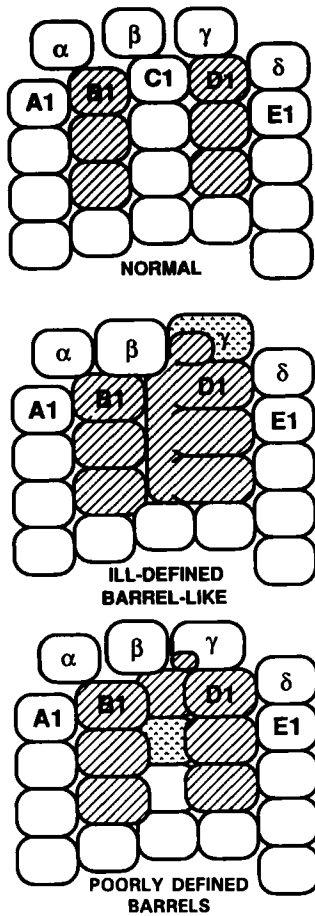


FIG. 6. Correlation of morphological and metabolic whisker maps in normal and altered barrel cortex. The schemata illustrate the structure-function relationships in unoperated controls (top), in animals in which the lesion caused the development of an ill-defined barrel-like disorganized zone (centre), and in animals in which the lesion led to a disorganized zone containing poorly defined barrels (bottom). The pattern of neural metabolic activation, evoked by the stimulation of whiskers B1-3 and D1-3, is superimposed on the barrel pattern. Rounded rectangles depict barrels, or barrel-like structures, and the disorganized zone. The barrels of the straddlers and the most posterior barrel in each row are labelled (orientation: caudal is up, medial is right). Considering all results of a given group, each area is assigned a degree of activation: low as in barrels A1-3 and E1-3 (blank), intermediate (stippled), and high as in barrels B1-3 and D1-3 (hatched). The degree of activation is weighted by the frequency at which the area was activated. In mice with an ill-defined barrel-like disorganized zone, barrel  $\gamma$  and barrels in row D could not be separated from the zone, and the demarcation lines are, therefore, omitted in the centre scheme. In the bottom scheme, the disorganized zone is composed of poorly defined barrels represented by partially hidden rounded rectangles. Unlike the convergence between the metabolic and the morphological whisker map in normal barrel cortex, the maps diverge in the two types of altered neocortex, and the pattern of metabolic activation cannot be predicted from the morphological map.

cases, responsivity to stimulation was highest in layer IV, and the presence of afferents from the ventrobasal nucleus is supported by patches of high cytochrome oxidase activity. Activation of the disorganized zone may, therefore, stem from these thalamocortical afferents. Their terminal fields may have shrunk, however, leading to the thinning of layer IV in and near the disorganized zone indicated in sections stained for cytochrome oxidase activity.

The profound role of thalamocortical afferents in the plasticity of columnar functional cortical units as a consequence of lesions in the

sensory periphery has been firmly established for occlusion dominance columns in visual cortex. Occlusions of one eye briefly after birth results in an altered map in the primary visual cortex; the dominance columns subserved by the functional eye are enlarged at the expense of the representation of the deprived eye (Hubel *et al.*, 1977; DesRosiers *et al.*, 1978). In the newborn monkey thalamocortical afferents subserved by one eye terminate in partial overlap with the afferents from the other eye. During normal development the overlapping terminations are pruned until separate domains are established (LeVay *et al.*, 1980). Monocular deprivation interferes with this process. Analogously, we hypothesize that in barrel cortex the fields of termination of afferents from the ventrobasal nucleus connected to whisker follicles adjacent to the lesion enlarge at the expense of the terminal fields of afferents deprived by the lesion.

The location of the disorganized zone in barrel cortex corresponds topologically to the location of the lesion on the snout and its associated tactile field. An object deflecting the whiskers adjacent to the lesion usually covers the tactile field over the lesion as well. The disorganized zone becomes activated by a disturbance in its corresponding tactile field. Therefore, reduced spatial specificity would provide the disorganized zone with the capacity to complement the tactile compound map of the whiskerpad. The observed responsivity in altered neocortex may reflect a true plastic compensation for functional loss. That neural responses in the disorganized zone were not restricted to the input layers of afferents from the ventrobasal nucleus but also occurred in the layers giving rise to cortico-cortical connections bolsters the hypothesis that the disorganized zone may play a role in the processing of somesthetic information.

*Comparison with other studies*

The effects of gross neonatal lesions of whisker follicles on the metabolic whisker map in barrel cortex have been studied by Kossut and Hand (1984). The investigators removed all whisker follicles but one on one side in rats on postnatal day 1 and stimulated that whisker and the corresponding whisker on the unoperated side in deoxyglucose studies between postnatal days 4 and 27. In harmony with the results of the present study the authors found that the deprivation resulted in an expansion of the area of activation in barrel cortex contralateral to the lesion. The metabolic representation of the surviving whisker continued to enlarge until adulthood.

Simons *et al.* (1984) and Durham and Woolsey (1985), employing a lesion paradigm similar to ours, observed no responsivity to whisker stimulation in the area intercalated between enlarged barrels that we designated as the 'disorganized zone'. In these two studies the whisker follicles in entire row C were electrocauterized in newborn rats and mice. In contrast, in the present study only three whisker follicles were removed. In spite of this difference, the morphological patterns of altered barrel cortex shown in the two studies as a result of early intervention are very similar to those described in the present study. Therefore, it is unlikely that the discrepancy in findings between the two studies and ours are due to the different number of destroyed whisker follicles. There are, however, essential methodological differences between these studies and ours. Using anaesthetized preparations, Simons *et al.* (1984) recorded from single units in the territory representing the site of the lesion, i.e. row C, in barrel cortex. The authors sampled a significant number of neurons unresponsive to whisker stimulation whereas the few responsive neurons encountered were 'hard to drive'. The authors concluded that this part of barrel cortex 'appears to be functionally disconnected from the sensory periphery' (Simons *et al.*, 1984). The recordings focused on the spiking of single neurons occurring in less than a second after the deflection of a whisker. In

the present study, however, rates of glucose utilization were averaged over entire barrels, and whiskers were repetitively stimulated for almost 1 h. The rates of glucose utilization reflect all neuronal responses in that period. Based on the methodological differences, discrepancies in results obtained with the quantitative deoxyglucose method and single-unit recordings are, therefore, not surprising.

In the other study employing the same type of lesion, Durham and Woolsey (1985) investigated neural activation related to whisker stimulation in mouse barrel cortex with a non-quantitative modification of the deoxyglucose method. [<sup>3</sup>H]Deoxyglucose was used as a tracer in an effort to achieve cellular resolution. In this procedure ~95% of the label is washed out of the brain tissue (Durham *et al.*, 1981). Stimulation of whiskers adjacent to the lesion increased tracer accumulation only slightly in the disorganized zone. The authors concluded that, in agreement with the findings of Simons *et al.* (1984), the disorganized zone remained 'silent' to whisker stimulation. The discrepancy between the low tracer accumulation Durham and Woolsey (1985) found in the disorganized zone and the strong increase in rates of glucose utilization we found may be due to the loss of label endured for the sake of gaining spatial resolution. The radioactivity remaining in the tissue may have been selectively retained in glycogen rather than deoxyglucose-6-phosphate, and is probably a poor indicator of the rate of glucose utilization (Nelson *et al.*, 1984).

### Outlook

We found that the metabolic whisker map in adult mouse barrel cortex adapts to lesions of a limited number of whisker follicles inflicted shortly after birth. It would be of interest to determine if this functional reorganization is already present at the earliest age at which a metabolic whisker map can be observed. Should the alteration be absent at that time and evolve subsequently? Do whiskers adjacent to the lesion have to be functional in order to enlarge their metabolic representations into the deprived territory? Future experiments will be directed towards these important questions.

### Acknowledgements

We are indebted to Thao P. Dang, Y. Sun and K. Schmidt for their help in critical phases of the experiments, J. Jehle, V. TenEyck and E. Lewis for technical assistance, J. D. Brown for photography, E. M. Glaser, J. Glaser and A. Prescott for their help with reconstructions of the barrel cortex using NeuroLucida, and K. Pettigrew for her advice on statistical analysis. We are indebted to Professor Hendrik Van der Loos, Institute of Anatomy, University of Lausanne, Switzerland, for providing the stimulator, and to Professor Karl Georg Götz, Max-Planck-Institut für biologische Kybernetik, Tübingen, FRG, for providing the wire used for the deflection of the whiskers. We thank L. Sokoloff for many helpful comments and his unrelenting support. P. M. was supported by a Fogarty Fellowship.

### References

- Armstrong-James, M. (1975) The functional status and columnar organization of single cells responding to cutaneous stimulation in neonatal rat somatosensory cortex SI. *J. Physiol. (Lond.)*, **246**, 501–538.
- Armstrong-James, M. and Fox, K. (1987) Spatiotemporal convergence and divergence in the rat S1 "barrel" cortex. *J. Comp. Neurol.*, **263**, 265–281.
- Armstrong-James, M. and Callahan, C. (1991) Thalamocortical mechanisms in the formation of receptive fields of rat barrel cortex neurons. II. The contribution of ventroposterior medial thalamic (VPM) neurones. *J. Comp. Neurol.*, **303**, 211–224.
- Armstrong-James, M., Callahan, C. A. and Friedman, M. A. (1991) Thalamocortical processing of vibrissal information in the rat. I. Intracortical origins of surround but not centre-receptive fields of layer IV neurones in the rat S1 barrel cortex. *J. Comp. Neurol.*, **303**, 193–210.
- Bernardo, K. L. and Woolsey, T. A. (1987) Axonal trajectories between mouse somatosensory thalamus and cortex. *J. Comp. Neurol.*, **258**, 542–564.
- Bernardo, K. L., McCasland, J. S. and Woolsey, T. A. (1990a) Local axonal trajectories in mouse barrel cortex. *Exp. Brain Res.*, **82**, 247–253.
- Bernardo, K. L., McCasland, J. S., Woolsey, T. A. and Strominger, R. N. (1990b) Local intra- and interlaminar connections in mouse barrel cortex. *J. Comp. Neurol.*, **291**, 231–255.
- Chapin, J. K. and Lin, C.-S. (1984) Mapping the body representation in the SI cortex of anesthetized and awake rats. *J. Comp. Neurol.*, **229**, 199–213.
- Chapin, J. K., Sadeq, M. and Guise, J. L. U. (1987) Corticocortical connections within the primary somatosensory cortex of the rat. *J. Comp. Neurol.*, **263**, 326–346.
- Chmielowska, J., Kossut, M. and Chmielowski, M. (1986) Single vibrissal cortical column in the mouse labeled with 2-deoxyglucose. *Exp. Brain Res.*, **63**, 607–619.
- Cruz, M. C., Jeanmonod, D., Meier, K. and Van der Loos, H. (1984) A silver and gold technique for axons and axon-bundles in formalin-fixed central and peripheral nervous tissue. *J. Neurosci. Methods*, **10**, 1–8.
- Des Rosiers, M. H., Sakurada, O., Jehle, J., Shinohara, M., Kennedy, C. and Sokoloff, L. (1978) Functional plasticity in the immature striate cortex of the monkey shown by the [<sup>14</sup>C]deoxyglucose method. *Science*, **200**, 447–449.
- Dörfl, J. (1985) The innervation of the mystacial region of the white mouse. A topographical study. *J. Anat.*, **142**, 173–184.
- Dubner, R. and Sessle, B. J. (1971) Presynaptic modification of corticofugal fibers participating in a feedback loop between trigeminal brainstem nuclei and sensorimotor cortex. In Dubner, R. and Kawamura, Y. (eds), *Oral-facial Sensory Motor Mechanisms*. Appleton-Century-Crofts Educational Division, Meredith Corporation, New York, NY, pp. 299–313.
- Durham, D. and Woolsey, T. A. (1977) Barrels and columnar organization: Evidence from 2-deoxyglucose (2-DG) experiments. *Brain Res.*, **137**, 169–174.
- Durham, D. and Woolsey, T. A. (1984) Effects of neonatal whisker lesions on mouse central trigeminal pathway. *J. Comp. Neurol.*, **223**, 424–447.
- Durham, D. and Woolsey, T. A. (1985) Functional organization in cortical barrels of normal and vibrissae-damaged mice: A (<sup>3</sup>H)2-deoxyglucose study. *J. Comp. Neurol.*, **235**, 97–110.
- Durham, D., Woolsey, T. A. and Kruger, L. (1981) Cellular localization of 2-[<sup>3</sup>H]deoxy-D-glucose from paraffin-embedded brains. *J. Neurosci.*, **1**, 519–526.
- Elhanany, E. and White, E. L. (1990) Intrinsic circuitry: Synapses involving the local axon collaterals of cortical projection neurons in the mouse primary somatosensory cortex. *J. Comp. Neurol.*, **291**, 43–54.
- Hand, P. J. (1981) The deoxyglucose method. In Heimer, L. and Robards, M. J. (eds), *Neuroanatomical Tract-tracing Methods*. Plenum Press, New York, NY, pp. 511–538.
- Hubel, D. H., Wiesel, T. N. and LeVay, S. (1977) Plasticity of ocular dominance columns in monkey striate cortex. *Phil. Trans. Roy. Soc. Lond. Ser. B*, **278**, 377–409.
- Ito, M. (1985) Processing of vibrissa sensory information within the rat neocortex. *J. Neurophysiol.*, **54**, 479–490.
- Jeanmonod, D., Rice, F. L. and Van der Loos, H. (1981) Mouse somatosensory cortex: Alterations in the barrelfield following receptor injury at different early postnatal ages. *Neuroscience*, **6**, 1503–1535.
- Jensen, K. F. and Killackey, H. P. (1987) Terminal arbors projecting to the somatosensory cortex of the adult rat. I. The normal morphology of specific thalamocortical afferents. *J. Neurosci.*, **7**, 3529–3543.
- Kadekaro, M., Crane, A.M. and Sokoloff, L. (1985) Differential effects of electrical stimulation of sciatic nerve on metabolic activity in spinal cord and dorsal root ganglion in the rat. *Proc. Natl. Acad. Sci. USA*, **82**, 6010–6013.
- Keller, A. and White, E. L. (1987) Synaptic organization of GABAergic neurons to cortical barrels in the rat. *Brain Res.*, **51**, 326–331.
- Killackey, H. P. and Belford, G. R. (1979) The formation of afferent patterns in the somatosensory cortex of the neonatal rat. *J. Comp. Neurol.*, **183**, 285–304.
- Killackey, H. P. and Leshin, S. (1975) The organization of specific thalamocortical projections to the posteromedial barrel subfield of the rat somatic sensory cortex. *Brain Res.*, **86**, 469–472.
- Kossut, M. and Hand, P. (1984) Early development of changes in cortical representation of C3 vibrissa following neonatal denervation of surrounding vibrissa receptors: A 2-deoxyglucose study in the rat. *Neurosci. Lett.*, **46**, 7–12.
- LeVay, S., Wiesel, T. N. and Hubel, D. H. (1980) The development of ocular dominance columns in normal and visually deprived monkeys. *J. Comp. Neurol.*, **191**, 1–51.
- Lorente de N6, R. (1922) La corteza cerebral del rat6n. *Trab. Lab. Invest. Biol. Univ. Madrid*, **20**, 41–78.

- Melzer, P., Van der Loos, H., Dörfl, J., Welker, E., Robert, P., Emery, D. and Berrini, J.-C. (1985) A magnetic device to stimulate selected whiskers of freely moving or restrained small rodents: its application in a deoxyglucose study. *Brain Res.*, **348**, 229–240.
- Nelson, T., Kaufman, E. E. and Sokoloff, L. (1984) 2-Deoxyglucose incorporation into rat brain glycogen during measurement of local cerebral glucose utilization by the deoxyglucose method. *J. Neurochem.*, **43**, 949–956.
- Nussbaumer, J.-C. and Van der Loos, H. (1985) An electrophysiological and anatomical study of projections to the mouse cortical barrelfield and its surroundings. *J. Neurophysiol.*, **53**, 686–698.
- Rice, F. L. and Van der Loos, H. (1977) Development of the barrels and barrel field in the somatosensory cortex of the mouse. *J. Comp. Neurol.*, **171**, 545–560.
- Rice, F. L., Mance, A. and Munger, B. L. (1986) A comparative light microscopic analysis of the sensory innervation of the mystacial pad. I. Innervation of vibrissal follicle–sinus complexes. *J. Comp. Neurol.*, **252**, 154–174.
- Senft, S. S. and Woolsey, T. A. (1991) Growth of thalamic afferents into mouse barrel cortex. *Cereb. Cortex*, **1**, 308–335.
- Sessle, B. J. and Dubner, R. (1971) Presynaptic depolarization and hyperpolarization of trigeminal primary and thalamic afferents. In Dubner, R. and Kawamura, Y. (eds), *Oral–facial Sensory Motor Mechanisms*. Appleton–Century–Crofts Educational Division, Meredith Corporation, New York, NY, pp. 279–297.
- Simons, D. J. (1978) Response properties of vibrissa units in the rat SI somatosensory cortex. *J. Neurophysiol.*, **51**, 798–820.
- Simons, D. J. (1985) Temporal and spatial integration in the rat SI vibrissa cortex. *J. Neurophysiol.*, **54**, 615–636.
- Simons, D. J. and Carvell, G. E. (1989) Thalamocortical response transformation in the rat vibrissa/barrel system. *J. Neurophysiol.*, **61**, 311–330.
- Simons, D. J., Durham, D. and Woolsey, T. A. (1984) Functional organization of mouse and rat SMI barrel cortex following vibrissal damage on different postnatal days. *Somatosensory Res.*, **1**, 207–245.
- Sokoloff, L. (1985) Application of quantitative autoradiography to the measurement of biochemical processes in vivo. In Reivich, M. and Alavi, A. (eds), *Positron Emission Tomography*. Alan R. Liss, New York, NY, pp. 1–42.
- Sokoloff, L., Reivich, M., Kennedy, C., Des Rosiers, D. H., Patlak, C. S., Pettigrew, K. D., Sakurada, O. and Shinohara, M. (1977) The [<sup>14</sup>C]deoxyglucose method for the measurement of local cerebral glucose utilization: Theory, procedure and normal values in the conscious and anesthetized albino rat. *J. Neurochem.*, **28**, 897–916.
- Steindler, D. A., O'Brien, T. F., Laywell, E., Harrington, K., Faissner, A. and Schachner, M. (1990) Boundaries during normal and abnormal brain development: *In vivo* and *in vitro* studies of glia and glycoconjugates. *Exp. Neurol.*, **109**, 35–56.
- Suda, S., Shinohara, M., Miyaoka, M., Lucignani, G., Kennedy, C. and Sokoloff, L. (1990) The lumped constant of the deoxyglucose method in hypoglycemia: Effects of moderate hypoglycemia on local cerebral glucose utilization in the rat. *J. Cereb. Blood Flow Metabol.*, **10**, 499–509.
- Van der Loos, H. (1976) Barreloids in mouse somatosensory thalamus. *Neurosci. Lett.*, **2**, 1–6.
- Van der Loos, H. and Woolsey, T. A. (1973) Somatosensory cortex: Structural alterations following early injury to sense organs. *Science*, **179**, 395–397.
- Welker, C. (1971) Microelectrode delineation of fine grain somatotopic organization of SMI cerebral cortex in albino rat. *Brain Res.*, **26**, 259–275.
- Welker, E., Rao, S. B., Dörfl, J., Melzer, P. and Van der Loos, H. (1992) Plasticity in the barrel cortex of the adult mouse: Effects of chronic stimulation upon deoxyglucose uptake in the behaving animal. *J. Neurosci.*, **12**, 153–170.
- White, E. L. and Keller, A. (1987) Intrinsic circuitry involving the local axon collaterals of corticothalamic projection cells in mouse SMI cortex. *J. Comp. Neurol.*, **262**, 13–26.
- Wong-Riley, M. T. T. (1979) Changes in the visual system of monocularly sutured or enucleated cats demonstrable with cytochrome oxidase histochemistry. *Brain Res.*, **171**, 11–28.
- Wong-Riley, M. T. T. and Welt, C. (1980) Histochemical changes in cytochrome oxidase of cortical barrels after vibrissal removal in neonatal and adult mice. *Proc. Natl Acad. Sci. USA*, **77**, 2333–2337.
- Woolsey, T. A. and Van der Loos, H. (1970) The structural organization of layer IV in the somatosensory region (SMI) of mouse cerebral cortex. The description of a cortical field composed of discrete cytoarchitectonic units. *Brain Res.*, **17**, 205–242.